

# Organic/Inorganic Nanocomposite Star Polymers via Atom Transfer Radical Polymerization of Methyl Methacrylate Using Octafunctional Silsesquioxane Cores

Ricardo O. R. Costa and Wander L. Vasconcelos

*Department of Metallurgical and Materials Engineering, Federal University of Minas Gerais, Belo Horizonte, MG, Brazil 30160-030*

Ryo Tamaki and Richard M. Laine\*

*Departments of Materials Science and Engineering, Chemistry and the Macromolecular Science and Engineering Center, University of Michigan, Ann Arbor, Michigan 48109-2136*

*Received May 10, 2001*

**ABSTRACT:** A method was developed for atom transfer radical polymerization (ATRP) synthesis of a nanocomposite consisting of dispersed, nanosized hard particles in a thermoplastic matrix. Octafunctional cubic silsesquioxanes were used as a platform to synthesize 8-arm star poly(methyl methacrylate) (PMMA) via ATRP. The cubic silsesquioxane, octakis(hydridodimethylsiloxy)octasilsesquioxane ( $Q_8M_8^{H_8}$ ), was converted to either octakis(2-bromo-2-methylpropionyloxypropyldimethylsiloxy)octasilsesquioxane (OBPS) or the octaethylbenzyl chloride analogue. The bromo ester was successfully employed as an ATRP initiator using CuCl as catalyst, leading to formation of PMMA arms with controlled molecular weights and hence to nanocomposites with essentially complete control of dispersion and solids loading. The catalyst and initiator concentrations were demonstrated to affect the molecular weight distribution and the occurrence of star–star coupling caused by inevitable termination reactions.

## Introduction

There is considerable interest in preparing nanocomposite materials with completely controlled architectures that can be tailored for specific technical applications or designed as model systems to better understand specific scientific principles. Extensive efforts have been made to control the synthesis and properties of organic/inorganic hybrid materials using for example polyhedral silsesquioxanes,<sup>1–3</sup> silica gel-derived hybrids,<sup>4,5</sup> and layered organic/inorganic nanocomposites.<sup>6</sup> Similar trends are observed when one considers all the work published on the synthesis of organic polymers with well-defined architectures. Many of these studies deal with different kinds of regular branched molecules (stars, combs, ladders, dendrimers).<sup>7–9</sup>

A great advantage of branched polymers is that they offer lower melt and solution viscosities than their linear analogues with identical molecular weights.<sup>10</sup> The presence of even a small fraction of long-chain branched molecules may also result in properties considerably different from those of a purely linear polymer, affecting crystallinity, melting point, glass transition temperature, intrinsic viscosity, and viscoelastic behavior.<sup>7</sup>

Star polymers constitute unique structures among the regular branched polymers since each molecule has only one branching point. Precise architectural control in polymers is essential because it affects their properties and morphology. Well-defined star polymers can be used as models to evaluate theories concerning the influence of molecular structure on polymer properties.<sup>10</sup> It is in this regard that we have sought to develop a well-defined entrée into cubic silsesquioxane cored star polymers.

We have recently described efforts<sup>2,11</sup> to develop organic/inorganic nanocomposites wherein cubic silsesquioxanes provide an exactly defined (1.2 nm diameter) hard particle to which as many as eight identical covalently bonded polymerizable functional groups can be appended. Our objective is to link the cubes by chemical reactions that lead to organic tethers between the cubes wherein the architecture of the tether can be carefully varied. In this manner, keeping the hard particle a constant, we hope to probe the effects of changes in the tether length, architecture, and density on the macroscopic properties (microporosity, tensile strength, fracture toughness, coefficients of thermal expansion, etc.) of the resulting nanocomposite. Our ultimate goal is to develop structure–processing–property relationships that allow us to predict and tailor nanocomposite properties.

To this end, we have developed routes to nanocomposites based on epoxy resin chemistry, ring-opening polymerization, hydrosilylation, methacrylate polymerization, and simple thermal oxidation. To date, the types of nanocomposites we have prepared and whose properties we have probed are all highly cross-linked.<sup>12,13</sup> While we have been able to demonstrate some rather novel materials properties using this approach, the lack of access to related thermoplastic analogues thwarts efforts to extend the concept to a large class of materials.

On the basis of efforts of Matyjaszewski et al., as well as other research groups, the opportunity arose to use cubic silsesquioxanes as a core for the synthesis of methyl methacrylate star polymers using atom transfer radical polymerization (ATRP), which in principle could provide star polymers with very well-defined chain lengths. In effect, the resulting materials would be nanocomposite thermoplastics wherein the density of hard particles (filler species) is closely defined by the

\* Corresponding author: e-mail talsdad@umich.edu, tel (734) 764-6203, fax (734) 763-4788.

arm length. Furthermore, because the cores are the initiation sites, the cubic “filler” cores will be completely dispersed in the thermoplastic matrix, hence avoiding the effects of clustering in properties analyses. We report here our efforts to successfully develop these novel types of nanocomposite materials. We note that the starting point is the same, the octahydroxypropyl cube, which we also used to make an octamethacrylate that provides access to thermoset methyl methacrylate nanocomposites.<sup>14</sup>

Essentially two methods are employed to synthesize star polymers: the “arm-first” method,<sup>15–17</sup> which links linear chains to a suitable core, and the “core-first” method,<sup>18,19</sup> which uses an active multifunctional core to initiate growth of polymer chains. A variation of the “arm-first” technique, the “nodule” method, involves cross-linking of arms by attaching a few terminal divinyl compounds.<sup>20</sup> However, in this case, samples with large fluctuations in functionality are obtained. The problem with the arm-first method is the difficulty of achieving 100% linkage of chains to the core because of the increasing steric hindrance caused by the already attached long chains. Although the “core-first” method offers the potential to avoid this problem due to easy access of the monomer to the active core sites, inefficient initiation will cause the same problem. Nevertheless, once initiation is overcome, the steric problems diminish as the chains grow, and the distances between the reactive centers increase.

To synthesize well-defined stars, the use of initiators with precise functionality is mandatory. Besides, regular star polymers cannot be successfully synthesized by means of conventional free radical polymerization, as it would inevitably result in cross-linked materials due to uncontrolled termination reactions. Thus, the first star polymers were synthesized by ionic polymerization techniques,<sup>9,21</sup> which are usually limited to a narrow variety of monomers and are very sensitive to impurities. Although the concept of controlled/living polymerization processes has long been known,<sup>22</sup> only recent advances allowed the development of controlled radical polymerization techniques,<sup>23</sup> particularly atom transfer radical polymerization (ATRP).<sup>24–26</sup>

In ATRP, the reaction is initiated by an alkyl halide activated by a copper catalyst, and termination reactions are mostly suppressed because a rapid equilibrium occurs between dormant and active propagating species. Different vinylic monomers, e.g., styrenes,<sup>27–29</sup> acrylates, and methacrylates,<sup>30–38</sup> have been successfully polymerized and copolymerized in a controlled fashion using ATRP techniques, providing polymers with low polydispersities.

Recent reports describe the ATRP-based synthesis of 4-, 6-, 8-, and even 12-arm star polymers using organic initiators and different transition metal catalysts.<sup>39–41</sup> The potential use of these materials as templates for the production of low dielectric constant thin films has also been described.<sup>41</sup> A recent review<sup>42</sup> shows that particular attention has been directed to the synthesis of star polymers initiated by inorganic cores. This trend arises from the general interest in combining potential applications of hybrid materials with the facility with which branched polymers can be processed.

A number of organic polymers and oligomers containing pendant polyhedral oligomeric silsesquioxanes (POSS) have now been synthesized and their properties described.<sup>43–45</sup> The use of octahydroxypropyl silsesquioxane<sup>46</sup> ( $T_8^H$ ) as

the core for the synthesis of star poly(isobutylene) (PBI) using the “arm-first” method has also been reported. Here, allyl-terminated PBI chains were reacted where coupled to the Si–H groups via hydrosilylation. This strategy yielded stars with at most five out of eight possible arms because of steric hindrance, and there was also uncontrolled core–core coupling caused by traces of water. This process was later employed as a technique to make stars with many PBI arms radiating from condensed cyclosiloxanes.<sup>47</sup> In other work targeting regular stars from POSS cores, efforts were made to minimize steric hindrance.<sup>48</sup> Thus, stars were synthesized using octakis(hydridodimethylsiloxy)octasilsesquioxane ( $Q_8M_8^H$ ), where the Si–H bonds are moved one O–Si bond away from the cubic core. In this case, the successful synthesis of 8-arm star PBI was possible, but reaction times as long as 144 h with 66% excess PBI were necessary to obtain 100% attachment. The number of arms attached to the core was found to be eight based on the  $M_w$  ratio between star and arms, not considering the effect of branching on the hydrodynamic properties and, consequently, on retention times in gel permeation chromatography (GPC).

In this paper, we report the synthesis of a star poly(methyl methacrylate) from a cubic silsesquioxane using the “core-first” method via ATRP. We describe the effects of variations in initiator and catalyst concentrations and also type of initiator on the molecular weight distributions of the polymers obtained. The resulting polymers offer most of the properties sought as discussed above.

## Experimental Section

**Materials.** Syntheses of octakis(hydridodimethylsiloxy)octasilsesquioxane ( $HSiMe_2O$ ) $Si_8O_{12}$  ( $Q_8M_8^H$ )<sup>49,50</sup> and octakis(3-hydroxypropyldimethylsiloxy)octasilsesquioxane (OHPS)<sup>14</sup> followed modified literature procedures. Toluene for hydrosilylation was distilled from sodium/benzophenone under  $N_2$ . 2-Bromo-2-methylpropionyl bromide (98% Aldrich) and vinylbenzyl chloride (97% Aldrich, mixture of meta and para isomers) were used as received. Methyl methacrylate (99%, Acros) and acetonitrile (99.5%, Aldrich) were distilled under  $N_2$  and stored in flasks sealed under  $N_2$ .  $CuCl$  (98%, Aldrich) was purified by stirring for 4 h with acetic acid, which dissolves  $CuCl_2$ . After filtration, it was washed with ethanol and dried. All other reagents and solvents were used as received from standard vendors.

**Characterization.** All  $^1H$  and  $^{13}C$  NMR were run in  $CDCl_3$  and recorded on a Varian Mercury 300 MHz NMR spectrometer.  $^{29}Si$  NMR spectra were recorded on a Bruker AM 360 NMR spectrometer operated at 71.5 MHz. All analyses by gel permeation chromatography (GPC) were performed on a Waters 440 system, using an Acuflo series III pump and Waters styragel columns ( $7.8 \times 300$ , HT2, 3, 4) with RI detection using an Optilab DSP interferometric refractometer (Wyatt Technology). The system was calibrated using polystyrene standards, the eluent was  $CH_2Cl_2$ , and the flow was 1.0 mL/min.

**Octakis(2-bromo-2-methylpropionoxypropyldimethylsiloxy)octasilsesquioxane (OBPS).** OHPS cube (3.00 g, 2.02 mmol) was added to a 50 mL Schlenk flask equipped with a magnetic stirrer.  $CH_2Cl_2$  (24.0 mL) was added to dissolve the cube, followed by 2.55 mL (18.2 mmol) of triethylamine to trap HBr. The flask was then immersed in a bath at  $-78^\circ C$  and allowed to equilibrate for 15 min. 2-Bromo-2-methylpropionyl bromide (2.25 mL, 18.2 mmol) was added at once under  $N_2$ , and a yellowish precipitate formed. After 3 h stirring, the mixture was filtered, and the solution was transferred to a separatory funnel and washed twice with distilled water. It was then washed two times with a 0.5 N NaOH solution and two times with brine. The solution was then dried over

anhydrous sodium sulfate and concentrated under vacuum. The product obtained after vacuum-drying at room temperature was a yellowish wax (3.4 g, 60%). Selected characterization data:  $^1\text{H NMR}$  (300 MHz,  $\text{CDCl}_3$ ,  $\text{CHCl}_3$  ref): 4.14 (t, 16H,  $\text{CH}_2\text{-O}$ ), 1.94 (s, 48H,  $(\text{CH}_3)_2\text{-C}(\text{Br})(\text{C}=\text{O})$ ), 1.73 (p, 16H,  $\text{CH}_2\text{-CH}_2\text{-CH}_2$ ), 0.66 (t, 16H,  $\text{CH}_2\text{-Si}$ ), 0.18 (s, 48H,  $(\text{CH}_3)_2\text{-Si}$ ).  $^{13}\text{C NMR}$  (75 MHz,  $\text{CDCl}_3$ ,  $\text{CHCl}_3$  ref): 171.8 ( $\text{C}=\text{O}$ ), 68.4 ( $\text{CH}_2\text{-O}$ ), 56.1 ( $\text{C}-\text{C}=\text{O}$ ), 31.0  $(\text{CH}_3)_2\text{C}(\text{Br})(\text{C}=\text{O})$ , 22.3 ( $\text{CH}_2\text{-CH}_2\text{-CH}_2$ ), 13.7 ( $\text{CH}_2\text{-Si}$ ), -0.1  $(\text{CH}_3)_2\text{-Si}$ .  $^{29}\text{Si NMR}$  (71.5 MHz,  $\text{CH}_2\text{Cl}_2$ , TMS ref): 12.0 ( $\text{O}(\text{Si}(\text{CH}_3)_2\text{CH}_2)$ ), -109.8 ( $\text{SiO}_4$ ). GPC analysis:  $M_n = 2050$ , PDI = 1.01.

**Octakis(2-(4-chloromethylphenyl)ethyl)dimethylsiloxy)-octasilsesquioxane (OCPS).**  $\text{Q}_8\text{M}_8^{\text{H}}$  (5.00 g, 4.91 mmol) was placed in a 100 mL Schlenk flask equipped with a reflux condenser and a magnetic stirrer. The reaction flask was carefully degassed and purged three times with  $\text{N}_2$ . Dry toluene (30 mL) was added followed by 7.0 mL (49.1 mmol) of vinylbenzyl chloride.  $\text{Pt}(\text{dvs})$  (2.0 mL of a 2 mM solution in toluene) was added. After  $\sim 15$  min the flask became slightly warm. The reacting solution was stirred for 4 h, and then triphenylphosphine ( $\sim 2$  mg) was added. The solution was concentrated to half of its original volume and then purified by precipitation in methanol. A clear viscous liquid (6.4 g, 58%) was obtained after vacuum-drying at  $40^\circ\text{C}$  for 4 h. According to  $^1\text{H NMR}$ , the reaction generated 55% of the  $\beta$ -adduct and 45% of the  $\alpha$ -adduct. Selected characterization data:  $^1\text{H NMR}$  (300 MHz,  $\text{CDCl}_3$ ,  $\text{CHCl}_3$  ref): 7.23 (m, 24H, aromatic  $\text{CH}$ ), 4.52 (s, 16H,  $\text{CH}_2\text{Cl}$ ), 2.66 (br, 8.8H,  $\text{CH}_2\text{-CH}_2\text{-Ar}$ ,  $\beta$ ), 2.25 (br, 3.6H,  $\text{Si-CH}(\text{CH}_3)\text{-Ar}$ ,  $\alpha$ ), 1.39 (br, 10.8H,  $\text{Si-CH}(\text{CH}_3)\text{-Ar}$ ,  $\alpha$ ), 0.95 (br, 8.8H,  $\text{Si-CH}_2\text{-CH}_2$ ,  $\beta$ ), 0.16 (s, 21.6H,  $(\text{CH}_3)_2\text{-Si-CH}$ ,  $\alpha$ ), 0.05 (s, 26.4H,  $(\text{CH}_3)_2\text{-Si-CH}_2$ ,  $\beta$ ). GPC analysis:  $M_n = 1770$ , PDI = 1.01.

**General Procedure for the Solution ATRP of Methyl Methacrylate.** In a typical reaction, 0.093 g (0.935 mmol) of  $\text{CuCl}$  and 0.438 g (2.80 mmol) of 2,2'-bipyridine were added to a 50 mL Schlenk flask, equipped with a reflux condenser and a magnetic stirrer. The reaction flask was carefully degassed and purged three times with  $\text{N}_2$ . Acetonitrile (20.0 mL) was added by syringe with immediate formation of a dark red solution. Methyl methacrylate (10.0 mL, 93.5 mmol) was also injected, and the homogeneous solution was equilibrated in an oil bath thermostated at  $90 \pm 2^\circ\text{C}$  for  $\sim 10$  min. In another small flask, OBPS initiator (0.313 g, 0.117 mmol) was dissolved in acetonitrile after the flask was evacuated and purged three times with  $\text{N}_2$ . A total of 10 mL of acetonitrile was used to dissolve the initiator and rinse the flask as a way to avoid initiator loss. The start of the reaction was recorded at the moment the initiator was injected into the reaction flask.

Samples of the reaction solution were collected at specific time intervals and treated as follows. A total of  $\sim 4.0$  mL of solution was collected each time by syringe, and 2.5 mL was immediately poured into 20 mL of methanol to precipitate the polymer. The remaining 1.5 mL was divided into three small preweighed aluminum pans, and the mass of solution deposited in each pan was recorded. The high surface area in each pan allowed rapid cooling and irreversible precipitation of copper chloride, which ensured that reaction was interrupted. The pans were then dried at  $70^\circ\text{C}$  in a vacuum oven until mass change ceased. The final masses were used to determine monomer conversion; based on the amount of solvent, monomer, and nonvolatile compounds in the initial reacting solution, it was possible to calculate the maximum and minimum possible dried masses, thus calculating conversion. The precipitated fraction in methanol was separated from the dark red alcoholic solution and washed 2–3 times with pure methanol, which removed virtually all the remaining copper complex from the polymeric mass. The white mass obtained was vacuum-dried and used for GPC determination of molecular weight.

Molecular weights of individual arms were determined by dissolution of the core with HF. The star polymer (50 mg) was dissolved in 1.0 mL of acetonitrile with 50  $\mu\text{L}$  of concentrated HF. The mixture was stirred at room temperature for 15 h. Solvent was vacuum-evaporated, and the samples were analyzed by GPC.

## Results and Discussion

To obtain hybrid star polymers via atom transfer radical polymerization (ATRP),  $\alpha$ -bromide esters and benzyl chloride groups were attached to the cubic silsesquioxane,  $\text{Q}_8\text{M}_8^{\text{H}}$ . The utility of the resulting octafunctional initiators for ATRP of methyl methacrylate was assessed by exploring the effects of variations in reaction conditions on the molecular weights and polydispersities of the starlike materials produced and on the molecular weights and polydispersities of the arms produced. In the following sections, we first discuss the synthesis of the two octafunctional initiators, then efforts to optimize the kinetics of the ATRP processes, and finally the analysis of the resulting polymers and an assessment of the materials obtained.

**Initiator Syntheses.** Initial attempts to obtain octakis(2-bromo-2-methylpropionyloxy propyldimethylsiloxy)-octasilsesquioxane (OBPS) initiator for ATRP focused on the hydrosilylation of allyl-2-bromo-2-methylpropionate with  $\text{Q}_8\text{M}_8^{\text{H}}$  (Scheme 1). Unfortunately, the reaction does not go to completion even after 36 h at  $60^\circ\text{C}$  with quite high catalyst concentrations.  $^1\text{H NMR}$  results revealed that most of the allyl groups remained unreacted. According to the literature,<sup>51</sup> in some instances hydrosilylation is hampered by severe side reactions. We suspect that, in the present case, it is likely that the tertiary bromide at least partially exchanges with  $\text{Si-H}$  to form  $\text{Si-Br}$ .

A second approach to OBPS (Scheme 1) explored the reaction of octakis(3-hydroxypropyldimethylsiloxy)-octasilsesquioxane (OHPS) with 2-bromo-2-methylpropionyl bromide. After several attempts it was determined that the reaction works best if run at  $-78^\circ\text{C}$  with rapid addition of the bromo compound. This procedure minimized side reactions, thus reducing the amounts of high molecular weight byproduct to tolerable levels, as demonstrated by GPC (Figure 1). We suspect that the high molecular weight byproduct results from cleavage of the cube under the reaction conditions used.

Another potential multifunctional initiator for ATRP octakis[2-(4-chloromethyl-phenyl)ethyl]dimethylsiloxy]-octasilsesquioxane (OCPS) was synthesized as depicted in Scheme 2. The synthetic procedure is very simple but resulted in a mixture of  $\alpha$ - (45%) and  $\beta$ -silylated (55%) isomers according to  $^1\text{H NMR}$ . The synthesis was further complicated by the use of vinylbenzyl chloride that was a mixture of 30% meta and 70% para isomers. Hence, the structure of the resulting OCPS is quite complex as seen by the relatively broad peaks in the  $^1\text{H NMR}$ .

**Synthesis of Stars via ATRP.** All the polymerization reactions conducted in this work were carried out using  $\text{CuCl}$  as the catalyst and acetonitrile as solvent. It was recently reported<sup>32</sup> that combining a bromo initiator with  $\text{CuCl}$  catalyst leads to rapid halogen exchange wherein alkyl chlorides are formed preferentially over alkyl bromides. This is expected to lead to faster initiation, slower propagation, and, consequently, better control of Mn. Acetonitrile was used as solvent because it dissolves 2,2'-bipyridine readily, and the bipyridyl copper complex catalyst forms easily. Thus, the use of more complex ligands such as alkyl-substituted bipyridines<sup>30</sup> or the alkylpyridylmethanimines<sup>31</sup> to ensure homogeneous methyl methacrylate polymerization are obviated. Furthermore, the solubility of the 2,2'-bipyridine complex in polar solvents such as methanol makes possible virtually complete extraction of the

## Scheme 1. Synthesis of Octakis(2-bromo-2-methylpropionoxypropyldimethylsiloxy)octasilsesquioxane (OBPS)

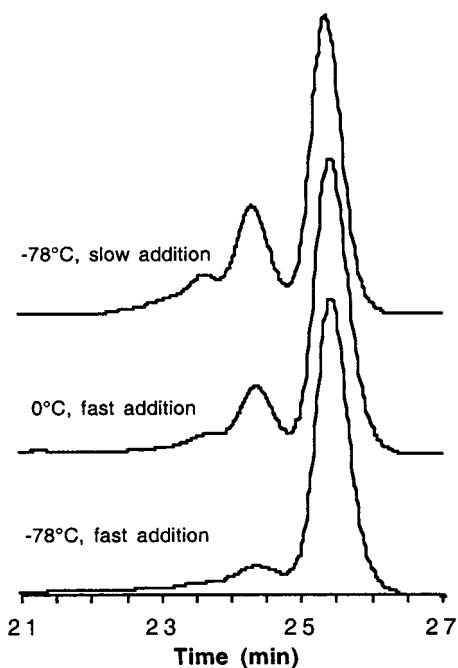
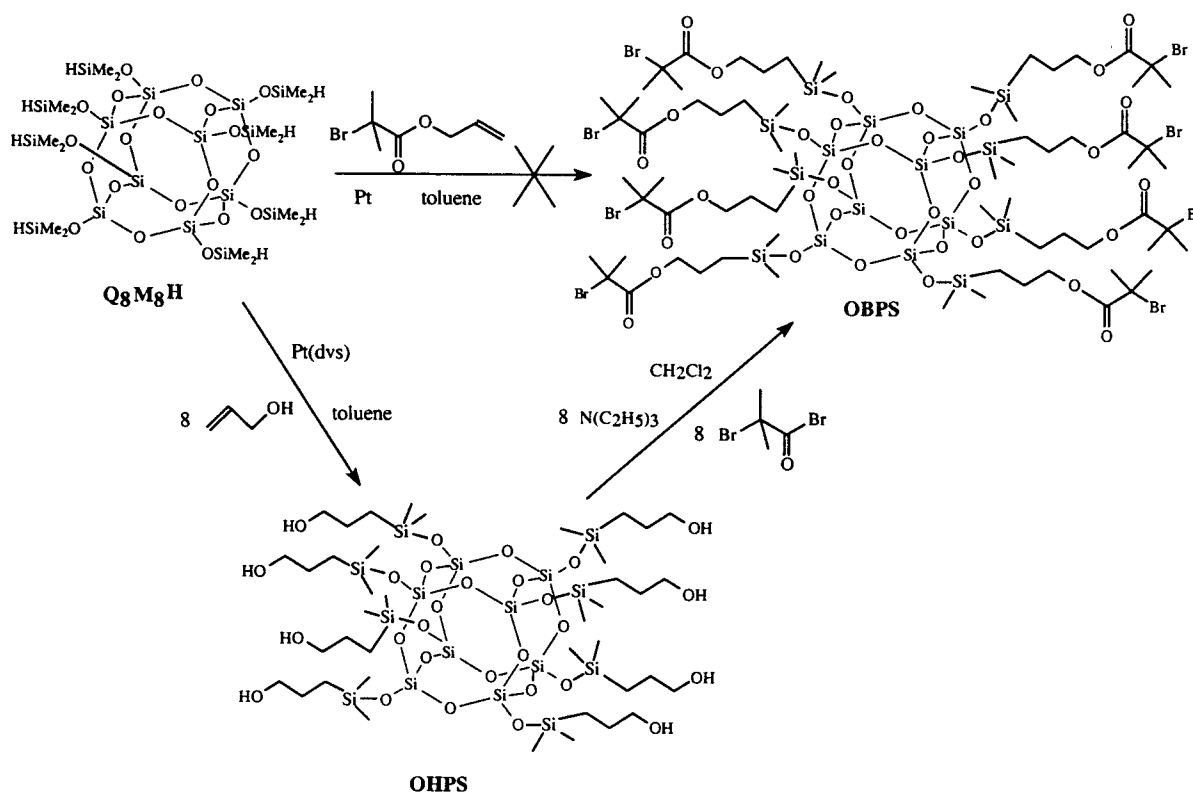


**Figure 1.** GPC traces of OBPS obtained under different reaction conditions.

copper complex via simple polymer precipitation. This works very well particularly in the case of PMMA and avoids the necessity of a further step of catalyst removal via column chromatography or ion exchange,<sup>52</sup> which is undesirable for industrial purposes. Polymer precipitation risks eliminating lower molecular weight species, which could compromise the results of these studies. However, targeting stars with higher molecular weights minimized this effect. Another advantage of the precipitation method is that it ensures the immediate

interruption of the reaction, generating more reliable results.

**OBPS Initiator Studies.** Four different studies (Table 1) were carried out using OBPS initiator. Figure 2 shows the dependence of the molecular weight of the star polymers on monomer conversion. The drawn lines represent the theoretical molecular weight,  $M_{n(th)}$ , calculated from

$$M_{n(th)} = (\text{conversion } \%) / 100 \cdot MW_M [M]_0 / [I]_0 + MW_I \quad (1)$$

where  $MW_M$  and  $MW_I$  are the molecular weights of the monomer and initiator, respectively, and  $[M]_0/[I]_0$  is the initial monomer-to-initiator molar ratio.

Studies (a) and (b) have the same theoretical line because they differ only in catalyst concentration. Their experimental molecular weights ( $M_n$ ) are reasonably coincident, which means that, under the conditions studied, copper concentration does not affect  $M_n$  itself, although it may affect the molecular weight distribution and the reaction kinetics. Molecular weights of systems (c) and (d) also show linear dependence on monomer conversion and the shifts in their magnitudes are correctly related to the initial monomer to initiator molar ratio. As can be seen, the data for runs (a) and (b) are slightly above theory. These results imply that either coupling reactions between star molecules occur to some extent or the initiator groups may have a limited efficiency.

Actually, the molecular weights of star polymers were expected to be lower than the theoretical ones. That is because the radius of gyration of a star molecule is smaller than that of a linear molecule with the same molecular weight due to the packing of the chains attached to the same core.<sup>10</sup> Therefore, the hydrodynamic properties are affected, and GPC analyses based

**Scheme 2. Synthesis of Octakis(2-(4-chloromethylphenyl)ethyl)dimethylsiloxy)octasilsesquioxane (OCPS);  $\beta$ -Silylated and Para Isomers Are Prevalent**

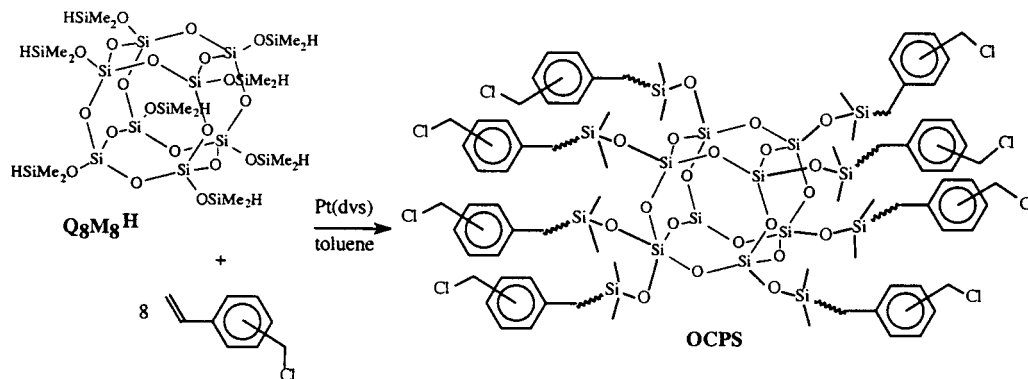


**Table 1. Reaction Conditions Tested for the Synthesis of Star PMMA in Acetonitrile at 90 °C Using Different Octafunctional Initiators**

study	OBPS (mM)	OCPS (mM)	CuCl (mM)	mol ratio ligand/CuCl	mol ratio MMA/(–Br or –Cl)	mol ratio CuCl/(–Br or –Cl)
(a)	2.92		23.4	3	100	1
(b)	2.92		46.8	3	100	2
(c)	5.84		23.4	3	50	0.5
(d)	1.46		11.7	3	200	1
(e)		2.92	23.4	3	100	1
(f)		2.92	46.8	3	100	2
(g)		5.84	46.8	3	50	1

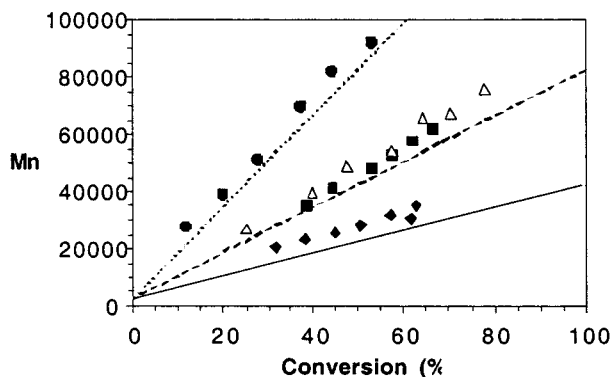


**Figure 2.** Dependence of molecular weights of star PMMA initiated by OBPS on monomer conversion for different reaction conditions. Lines represent the theoretical  $M_n$  for each experiment. ■: (a) [OBPS] = 2.92 mM, [CuCl] = 23.4 mM; △: (b) [OBPS] = 2.92 mM, [CuCl] = 46.8 mM; ◆: (c) [OBPS] = 5.84 mM, [CuCl] = 23.4 mM; ●: (d) [OBPS] = 1.46 mM, [CuCl] = 11.7 mM. For detailed conditions of studies (a), (b), (c) and (d), refer to Table 1.

on linear polystyrene standards give molecular weights lower than expected, causing the experimental data to shift to the region below the theoretical line.

In typical ATRP, the concentration of active species remains constant throughout the reaction, which can be verified by obtaining linear semilogarithmic plots of monomer conversion vs time. In all the experiments carried out, this dependence is not linear (Figure 3), or may be linear only in early stages of the reaction, for conversions <20%. The observed behavior can be explained by the occurrence of star–star coupling resulting from inevitable termination reactions. The dependence is probably linear early in the reaction, but the tendency for coupling increases with time, as monomer is depleted. As termination reactions occur, the number of active sites decreases, which partially explains the decreasing rate of polymerization. But more importantly, some portion of the CuX catalyst deactivates by

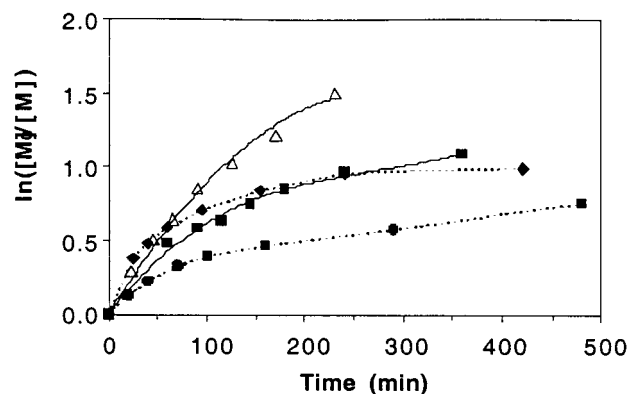


**Figure 3.** Semilogarithmic kinetic plot for the synthesis of star PMMA initiated by OBPS under different reaction conditions. Lines are used only to guide the eye. ■: (a) [OBPS] = 2.92 mM, [CuCl] = 23.4 mM; △: (b) [OBPS] = 2.92 mM, [CuCl] = 46.8 mM; ◆: (c) [OBPS] = 5.84 mM, [CuCl] = 23.4 mM; ●: (d) [OBPS] = 1.46 mM, [CuCl] = 11.7 mM. For detailed conditions of studies (a), (b), (c) and (d), refer to Table 1.

oxidization to CuX<sub>2</sub> due to elimination of active sites. Because of this “catalyst poisoning”, the maximum monomer conversion was ~66% in study (a). However, by increasing the initial CuCl concentration [study (b)], monomer conversions of almost 80% were reached in a much shorter time. It can also be observed that increases in initiator concentration [study (c)] lowered the maximum conversion slightly compared with study (a), although the initial propagation rate was higher. This is due to increases in star–star coupling caused by higher concentrations of star molecules.

The presence of higher molecular weight species derived from star–star coupling can be observed in the chromatograms obtained for study (d) (Figure 4). Under these specific reaction conditions, the higher molecular weight shoulder appears more clearly for conversions as low as 20% and increases with conversion for the reasons already mentioned. Visually, there appears to

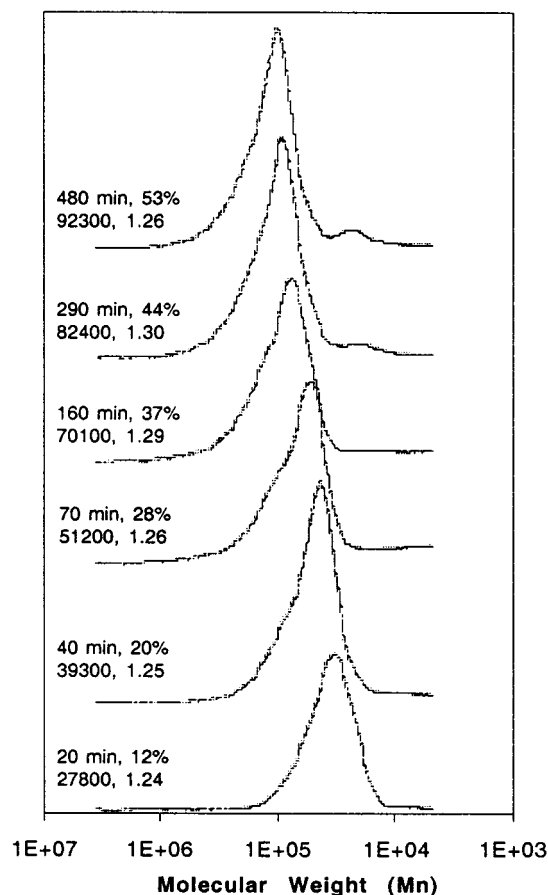


**Figure 4.** GPC traces of star polymers obtained from experiment (d): [OBPS] = 1.46 mM, [CuCl] = 11.7 mM. Values represent reaction time, MMA conversion,  $M_n$ , and PDI.

be a tendency for the shoulder to decrease at higher monomer conversions, but polydispersity (PDI) values increase slightly throughout the reaction. Considering both mechanisms for chain termination, disproportionation would first provide unsaturated chain ends that might lead to further coupling of stars, while radical combination would result in direct star–star coupling. The appearance of a lower molecular weight peak, which increases in intensity and molecular weight as the reaction proceeds, is also seen. This effect is more clearly observed in Figure 5, where the chromatograms for study (b) are presented. In this case, the catalyst concentration was much higher than in the previous case (Table 1). The lower molecular weight species probably arise from transfer reactions, which are enhanced by the longer average radical lifetime resulting from increases in catalyst concentration. High concentration of CuCl also promotes the formation of small amounts of species with extremely high molecular weights, which can be attributed to higher order coupling between the stars.

The effect of catalyst and initiator concentration on the molecular weight distribution can be observed in Figure 6. Although PDI values are usually 1.1–1.2 for a typical ATRP, the star polymers synthesized here have slightly higher PDIs, likely because of star–star coupling and the characteristics of the OBPS initiator synthesized, which contains a small fraction of a higher  $M_n$  compound (Figure 1). If one termination event causes two arms of different 8-arm star molecules to couple, the other 14 propagating chains are indirectly involved in this event, which means that the polydis-

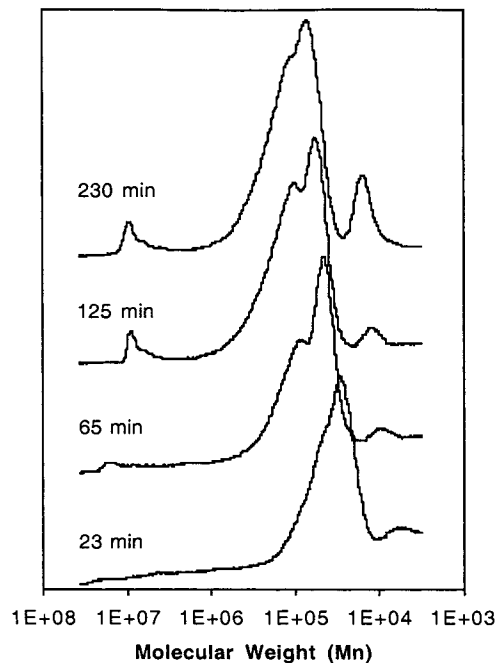


**Figure 5.** GPC traces of star polymers obtained from experiment (b), collected at different reaction times. [OBPS] = 2.92 mM, [CuCl] = 46.8 mM.

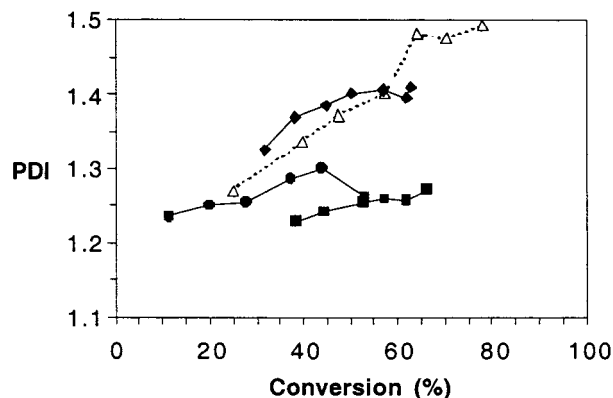


**Figure 6.** Dependence of polydispersity (PDI) on monomer conversion for the synthesis of star PMMA initiated by OBPS, under different reaction conditions. Lines are used only to guide the eye. ■: (a) [OBPS] = 2.92 mM, [CuCl] = 23.4 mM; △: (b) [OBPS] = 2.92 mM, [CuCl] = 46.8 mM; ◆: (c) [OBPS] = 5.84 mM, [CuCl] = 23.4 mM; ●: (d) [OBPS] = 1.46 mM, [CuCl] = 11.7 mM. For detailed conditions of studies (a), (b), (c) and (d), refer to Table 1.

persity is more affected in star systems. As expected, the increase of PDI with monomer conversion is larger for higher catalyst [study (b)] and initiator [study (c)] concentrations. When catalyst concentration is increased, the average radical lifetime is also increased, and termination reactions are more likely to occur. On the other hand, when initiator concentration is increased, the probability for termination reactions increases because of the higher concentration of active stars present in the reaction medium. Both factors generate polymers with broader  $M_n$  distributions.

Figure 7 shows the chromatograms of selected samples with similar molecular weights but generated under different reaction conditions. Samples generated under conditions (b) and (c) present slightly broader distributions, indicating that high catalyst or initiator concentrations lead to more polydisperse materials. One pertinent comment on Figure 7 is that optimum reaction

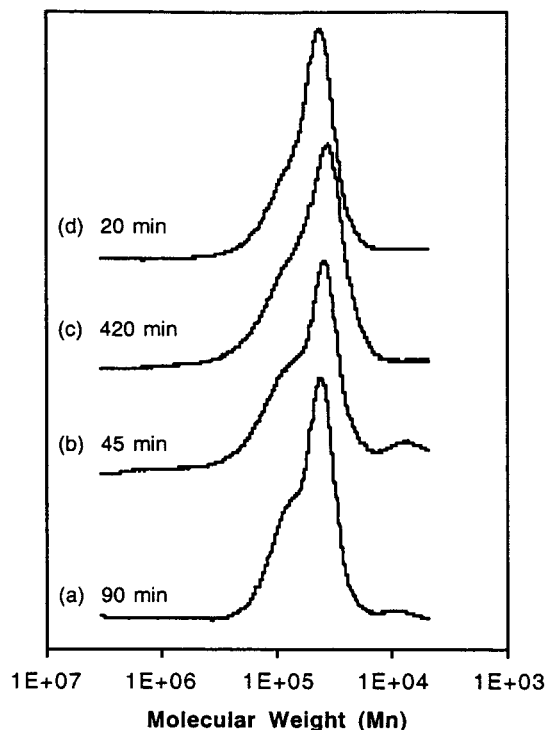


**Figure 7.** GPC traces of star polymer with similar  $M_n$  but obtained under different reaction conditions: (a) [OBPS] = 2.92 mM, [CuCl] = 23.4 mM; (b) [OBPS] = 2.92 mM, [CuCl] = 46.8 mM; (c) [OBPS] = 5.84 mM, [CuCl] = 23.4 mM; (d) [OBPS] = 1.46 mM, [CuCl] = 11.7 mM. For detailed conditions of studies (a), (b), (c) and (d), refer to Table 1.

conditions can be established for the synthesis of stars with a predetermined molecular weight by simply controlling basic reaction parameters and interrupting the polymerization at the appropriate time. Unfortunately, it seems that longer reaction times and low monomer conversions are required to obtain better control of the star architecture. These reaction parameters are quite important because they permit us to generate thermoplastic nanocomposites with the highest degree of control of dispersion and hence of mechanical properties.

**Determination of the Number of Arms.** To verify the above comments, it was important to determine the actual number of polymeric chains attached to the core. The cubes offer a unique opportunity to do this because the arms can be “liberated” from the core by cleaving the siloxane bonds of the cubic silsesquioxane with concentrated HF. Figure 8 compares the molecular weight of the stars and respective released arms as determined by GPC for study (a). One simple way to determine the number of arms would be to divide  $M_n$  of the star by the  $M_n$  of the arms, which would yield an approximate number of arms.

This ratio varies throughout the reactions from 6.2 to 6.7 for study (a) and 6.6 to 7.0 for study (d), which means that the number of arms is slightly below the maximum of eight arms possible. The problem with this calculation is that, as noted above, the molecular weight of a star molecule determined by GPC is lower than the actual one due to its smaller hydrodynamic volume. Besides, once the silsesquioxane is cleaved, this reasonably high molecular weight structure precipitates as silica gel. If not taken into account, both factors would contribute to give an incorrect estimate of the number of arms.

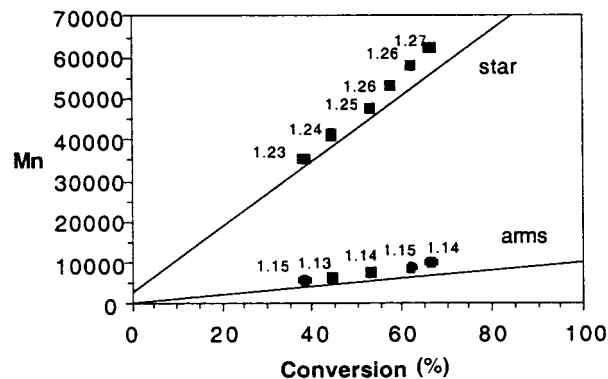


**Figure 8.** Comparison between  $M_n$  of star polymers (■) and the respective released arms (●) for study (a): [OBPS] = 2.92 mM, [CuCl] = 23.4 mM. Lines represent the theoretical  $M_n$ , and numbers are PDI values according to GPC.

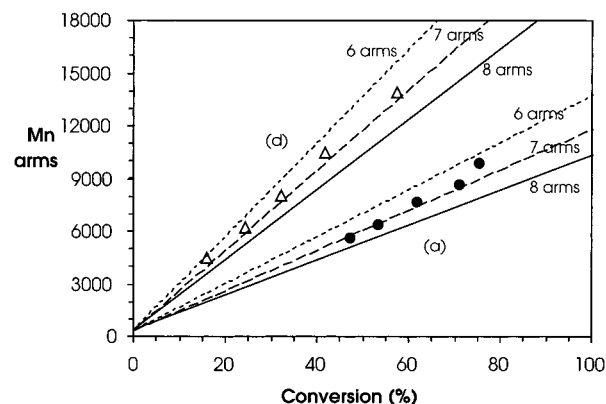


**Figure 9.** Dependence of molecular weights of the PMMA arms released from the core on monomer conversion for studies (a) and (d). ●: (a) [OBPS] = 2.92 mM, [CuCl] = 23.4 mM; △: (d) [OBPS] = 1.46 mM, [CuCl] = 11.7 mM. Lines represent the theoretical  $M_n$  of the arms assuming the stars have 8, 7, 6, or 5 arms.

A more precise way to determine the number of arms is to compare the experimental  $M_n$  of the arms with their theoretical  $M_n$  calculated on the basis of the initial monomer to initiator group ( $-\text{Br}$ ) molar ratio. If by any chance the initiator groups are inefficient to some degree, only some of the eight initiation sites for each macroinitiator would really generate arms, and consequently, the  $M_n$  of the arms would be higher. So, in Figure 9, the drawn lines represent the theoretical  $M_n$  of the arms assuming that the stars have 5, 6, 7, or 8 arms. The experimental data refer to the arms released from the star polymers synthesized in studies (a) and (d). The study (d) data are best simulated by the 6-arm theoretical line, with a tendency toward the 7-arm line for higher conversions.

In study (a), the trend is more likely to follow the 6-arm theoretical line independent of the conversion. Systems where the number of arms appears to be fewer than eight do not necessarily mean initiation inefficiency but could also result from some coupling reactions between well-defined 8-arm star molecules in the early stages of polymerization. Star–star coupling will impede propagation of one or two arms, thus increasing the  $M_n$  of the remaining propagating arms.

Since the concentration of stars in study (d) is lower than (a), the coupling effect is less pronounced, as seen in Figure 7, where a nearly bimodal molecular weight distribution for study (a) contrasts with the exhibition

of only a small shoulder for study (d). Therefore, data points referring to study (d) approach the 7-arm theoretical line at high conversions, while the average number of arms for study (a) persist around six. However, for the same reason, the data points for study (d) should also be closer to the 8-arm theoretical line at low conversions, which does not happen. But, considering that the CuCl:Br molar ratio was maintained at 1:1 for both studies (a) and (d), the fact that catalyst concentration was lower for study (d) may have affected the initiation efficiency in the early stages of polymerization, causing the generation of stars with "missing arms".

Star–star coupling generates 14-arm double stars, with cores linked by polymer chains of different sizes, depending on the stage of the reaction when coupling occurs. The final product probably consists of a distribution of different star sizes, including single 8-arm stars, a few single stars with "missing arms", and double or even triple stars, leading to an average of 6–7 arms per core. Other data that contribute to the star–star coupling hypothesis are the higher PDI for stars than for the released arms (Figure 8). Theoretically, when linear chains are linked to form stars with constant functionality, narrowing of the molecular weight distribution occurs,<sup>10</sup> which means that the PDI of the stars should be lower than the PDI of the arms. However, if double stars are formed, there is a sudden increase in PDI because the  $M_n$  doubles instantly, whereas the PDI of the arms remains unchanged at the moment of the coupling and increases slowly as the reaction proceeds.

There are some sources of error that could affect the experimentally determined  $M_n$ , leading to small deviations from what has been discussed. First, the system was calibrated using polystyrene standards, not PMMA standards; second, some hydrolysis of the polymer might occur because of the HF treatment. Although PMMA hydrolysis would not cause any fragmentation of the backbone structure, the molecular weight would be changed slightly by replacing CH<sub>3</sub> with OH groups and because the different chemical structures could also affect GPC retention times. To avoid this problem, the reaction was first tried with an equivalent amount of concentrated H<sub>2</sub>SO<sub>4</sub> because the lower water content could diminish the risk of PMMA hydrolysis. However, as observed in Figure 10, the molecular weight of the H<sub>2</sub>SO<sub>4</sub> treated product was higher than that resulting from HF treatment. Although the original star completely disappeared, the higher  $M_n$  means that core cleavage was incomplete, with some unbroken Si–O–Si bonds linking a few arms. On the other hand, GPC analysis of HF treated samples show only full stars and completely released arms, not intermediate species. This may be because, once the first core Si–O bond is broken, the whole structure becomes much more susceptible to the nucleophilic F<sup>-</sup> attack than the remaining unreacted stars. This suggests that the polymer chains restrict access to the silsesquioxane core. It is important to note that the molecular weight of the arms released by HF does not change with time, at least for the first 15 h of reaction used as the standard time for this procedure. The constant  $M_n$  means that the arms are likely to be completely released and that no significant PMMA hydrolysis occurs within this time interval. In addition, <sup>1</sup>H NMR analysis shows that virtually no hydrolysis occurs during the first few hours of reaction, meaning that the Si–O bonds are more susceptible to F<sup>-</sup> anion

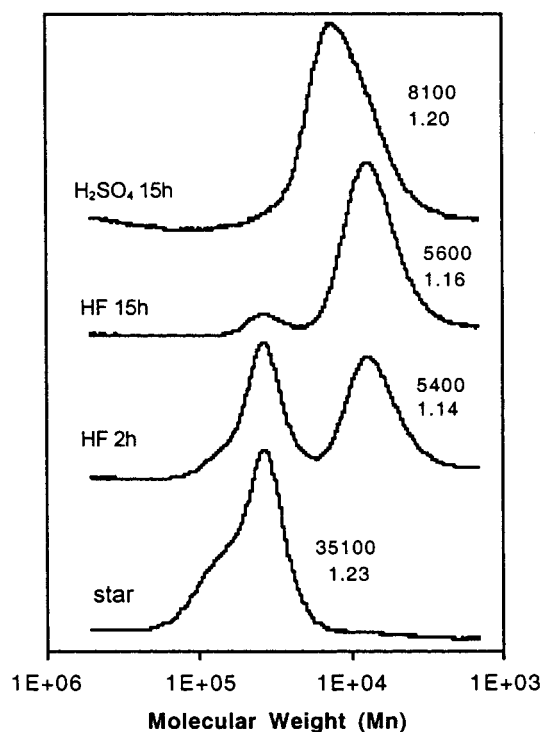


**Figure 10.** GPC traces of one star PMMA obtained from study (a) [OBPS] = 2.92 mM, [CuCl] = 23.4 mM and of the products resulting from reactions of the star with equivalent concentrations of HF and H<sub>2</sub>SO<sub>4</sub>. Values represent reaction time,  $M_n$ , and PDI.

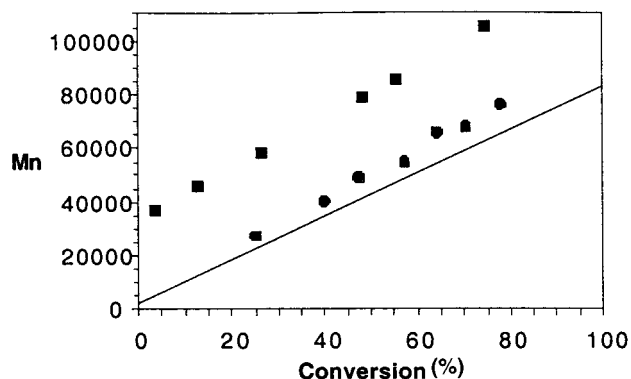


**Figure 11.** Comparison between the molecular weights of star polymers initiated by OCPS (■) or OBPS (●) under similar reaction conditions. Line represents the theoretical  $M_n$  for both studies; [initiator] = 2.92 mM, [CuCl] = 46.8 mM.

promoted cleavage than the ester groups to acid-catalyzed hydrolysis, under the reaction conditions used.

**OCPS Initiator Studies.** Additional experiments were carried out changing the type of initiator. Reaction conditions used for studies (a), (b), and (c) were reproduced (Table 1) with OCPS (Scheme 2) replacing OBPS initiator. Figure 11 compares the results obtained for study (f) (OCPS) with (b) (OBPS). The  $M_n$  of polymers initiated by OCPS are much higher than when OBPS is used, even at very low conversions. The most probable explanation is the low initiation efficiency of the benzyl chloride group for methyl methacrylate polymerization, as already reported in the literature.<sup>32</sup> Because only a few of the eight groups in each OCPS molecule are activated, only a few propagating arms result or maybe the star molecule does not even form.

The ratio between the  $M_n$  of the "star" and  $M_n$  of the "arms" was determined to be 1 for low conversions and

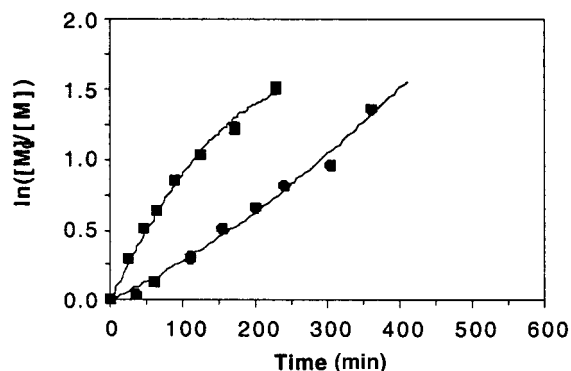


**Figure 12.** Semilogarithmic kinetic plot for the synthesis of star polymers initiated by OBPS [■, (b)] or OCPS [●, (f)] under similar reaction conditions. Lines are used only to guide the eye.

only  $\sim 2$  for conversions as high as 80%. This indicates that only 1–2 “arms” are attached to the OCPS core, and no star formation occurs. Thus, initiation is slower than propagation, and some additional initiation occurs as the reaction proceeds, but only a second “arm” forms. Statistically, species with one, two, and more arms must occur because of the high PDI values observed. However, at lower conversions, most initiator molecules are not reacted at all or have only one arm.

Figure 12 shows the semilogarithmic conversion vs time for one of the experiments compared with the results obtained with OBPS. The reaction initiated by OBPS is faster for low conversions but becomes slower as the reaction proceeds for the reasons already discussed. Since the concentration of active sites is roughly 8 times lower in OCPS system, the star–star coupling effect is diminished and catalyst deactivation is minimized. As a result, if the number of “arms” really increases with time, the concentration of active species also increases, which explains the slightly increasing slope observed for OCPS curve in Figure 12.

**Synthesis of Star Block Copolymers.** Preliminary tests were carried out using 2-hydroxyethyl methacrylate (HEMA) to form a star block copolymer with PMMA. In study (b), HEMA was injected into the reaction flask after 230 min of reaction, when MMA conversion was more than 90%. The “living” star PMMA was employed as a platform to build stars with a hydrophobic core and a hydrophilic shell. Approximately 2 h after HEMA addition, the resulting star poly(MMA-co-HEMA) no longer precipitated on addition of methanol, which demonstrates the hydrophilic character of the stars formed. A more detailed characterization of the samples obtained is still in progress, as it requires different conditions for GPC analysis.

## Conclusions

Given the above-described goals, we have learned to synthesize novel organic/inorganic hybrid stars from an octafunctional cubic silsesquioxane (OBPS) via ATRP of methyl methacrylate. By cleaving the core structure with HF, the average number of arms was determined to be 6–7. However, the occurrence of star–star coupling as a result of inevitable termination led to the formation of a product distribution probably containing double and triple stars, depending on the reaction conditions. In general, if the reaction is interrupted at low monomer conversions better-defined single stars with lower PDIs are formed, strongly suggesting that

it is possible to prepare thermoplastic PMMA/cube hybrid polymers with complete control of dispersion.

Further conclusions from the above studies include the fact that the use of higher CuCl concentrations increases termination and transfer rates, thereby promoting star–star coupling and the formation of low molecular weight species. Also, because of enhanced star–star coupling, increases in initiator concentration lead to more polydisperse samples. The use of low initiator concentrations with suitable CuCl:initiator molar ratios should optimize the architectural control of the stars obtained.

The initiator with benzyl chloride groups (OCPS) was not effective for initiating ATRP of methyl methacrylate. Preliminary synthesis of star block copolymers using 2-hydroxyethyl methacrylate demonstrated the living nature of the polymerization reactions.

Finally, mechanical studies that compare nanocomposite properties of PMMA stars of various arm lengths are planned for comparison with the thermoset PMMA polymers that can be made from the octamethyl methacrylate cube materials.

**Acknowledgment.** R.O.R.C. and W.L.V. gratefully acknowledge CAPES (Brazil) for the financial support. The authors also acknowledge partial support from Pfizer and from the Air Force Phillips Laboratories at Edwards Air Force Base for aspects of these studies.

## References and Notes

- (1) Laine, R. M.; Zhang, C.; Sellinger, A.; Viculis, L. *Appl. Organomet. Chem.* **1998**, *12*, 715.
- (2) Laine, R. M.; Asuncion, M.; Baliat, S.; Filho, N. L.; Dias; Harcup, J.; Sutorik, A. C.; Viculis, L.; Yee, A. F.; Zhang, C.; Zhu, Q. *MRS Symp. Ser.*; Klein, L., De Guire, M., Lorrain, F., Mark, J., Eds.; Dec 1999; Vol. 576, pp 3–14.
- (3) Provatas, A.; Matison, J. G. *Trends Polym. Sci.* **1997**, *5*, 327.
- (4) Mascia, L. *Trends Polym. Sci.* **1995**, *3*, 61.
- (5) Novak, B. M. *Adv. Mater.* **1993**, *5*, 442.
- (6) Weimer, M. W.; Chen, H.; Giannelis, E. P.; Sogah, D. Y. *J. Am. Chem. Soc.* **1999**, *121*, 1615.
- (7) Quirk, R. P.; Lee, Y.; Kim, J. In *Star and Hyperbranched Polymers*; Mishra, M. K., Kobayashi, S., Eds.; Marcel Dekker: New York, 1999; Chapter 1.
- (8) Hadjichristidis, N.; Pispas, S.; Pitsikalis, M.; Iatrou, H.; Vlahos, C. *Adv. Polym. Sci.* **1999**, *142*, 71.
- (9) Webster, O. *Science* **1991**, *251*, 887.
- (10) Roovers, J. In *Encyclopedia of Polymer Science and Engineering*, 2nd ed.; Kroschwitz, J. L., Ed.; Wiley: New York, 1985; Vol. 2, p 478.
- (11) (a) Laine, R. M.; Choi, J.; Lee, I. Organic/inorganic nanocomposites with completely defined interfacial interactions. *Adv. Mater.* **2001**, *13*, 800–803. (b) Choi, J.; Harcup, J.; Yee, A. F.; Zhu, Q.; Laine, R. M. Organic/inorganic hybrid composites from cubic silsesquioxanes. *J. Am. Chem. Soc.*, in press.
- (12) Lin, E. K.; Snyder, C. R.; Mopsik, F. I.; Wallace, W. E.; Wu, W. L.; Zhang, C. X.; Laine, R. M. In *Organic/Inorganic Hybrid Materials*, *MRS Symp. Ser.*; Laine, R. M., Sanchez, C., Brinker, C. J., Giannelis, E., Eds.; Dec 1998; Vol. 519, pp 15–20.
- (13) Soles, C. L.; Lin, E. K.; Wu, W.-L.; Zhang, C.; Laine, R. M. In *Organic/Inorganic Hybrid Materials*, *MRS Symp. Ser.*; Laine, R. M., Sanchez, C., Brinker, C. J., Eds.; Dec 2000, in press.
- (14) Zhang, C.; Laine, R. M. *J. Am. Chem. Soc.* **2000**, *122*, 6979.
- (15) David, B. A.; Kinning, D. J.; Thomas, E. L.; Fetters, L. J. *Macromolecules* **1986**, *19*, 215.
- (16) Hadjichristidis, N.; Guyot, A. N.; Fetters, L. J. *Macromolecules* **1978**, *11*, 668.
- (17) Morton, M.; Helminiak, T. E.; Gadkary, S. D.; Bueche, F. J. *Polym. Sci.* **1962**, *57*, 471.
- (18) Jacob, S.; Majoros, I.; Kennedy, J. P. *Macromolecules* **1996**, *29*, 8631.
- (19) Schappacher, M.; Deffieur, A. *Macromolecules* **1992**, *25*, 6744.
- (20) Zhang, X.; Xia, J.; Matyjaszewski, K. *Macromolecules* **2000**, *33*, 2340.

- (21) Charleux, B.; Faust, R. *Adv. Polym. Sci.* **1999**, *142*, 1.
- (22) Szwarc, M. *Nature* **1956**, *178*, 1168.
- (23) Mishra, M. K.; Yagci, Y. In *Handbook of Radical Vinyl Polymerization*; Marcel Dekker: New York, 1998; Chapter 10.
- (24) Wang, J.-S.; Matyjaszewski, K. *Macromolecules* **1995**, *28*, 7901.
- (25) Wang, J.-S.; Matyjaszewski, K. *J. Am. Chem. Soc.* **1995**, *117*, 5614.
- (26) Patten, T. E.; Xia, J.; Abernathy, T.; Matyjaszewski, K. *Science* **1996**, *272*, 866.
- (27) Matyjaszewski, K.; Patten, T. E.; Xia, J. *J. Am. Chem. Soc.* **1997**, *119*, 674.
- (28) DiRenzo, G. M.; Messerschmidt, M.; Mülhaupt, R. *Macromol. Rapid Commun.* **1998**, *19*, 318.
- (29) Matyjaszewski, K.; Beers, K. L.; Kern, A.; Gaynor, S. G. *J. Polym. Sci., Part A: Polym. Chem.* **1998**, *36*, 823.
- (30) Grimaud, T.; Matyjaszewski, K. *Macromolecules* **1997**, *30*, 2216.
- (31) Haddleton, D. M.; Crossman, M. C.; Dana, B. H.; Duncalf, D. J.; Heming, A. M.; Kukulj, D.; Shooter, A. J. *Macromolecules* **1999**, *32*, 2110.
- (32) Matyjaszewski, K.; Shipp, D. A.; Wang, J.-L.; Grimaud, T.; Patten, T. E. *Macromolecules* **1998**, *31*, 6836.
- (33) Roos, S. G.; Müller, A. H. E.; Matyjaszewski, K. *Macromolecules* **1999**, *32*, 8331.
- (34) Haddleton, D. M.; Jasieczek, C. B.; Hannon, M. J.; Shooter, A. J. *Macromolecules* **1997**, *30*, 2190.
- (35) Haddleton, D. M.; Kukulj, D.; Duncalf, D. J.; Heming, A. M.; Shooter, A. J. *Macromolecules* **1998**, *31*, 5201.
- (36) Haddleton, D. M.; Heming, A. M.; Kukulj, D.; Duncalf, D. J.; Shooter, A. J. *Macromolecules* **1998**, *31*, 2016.
- (37) Shipp, D. A.; Wang, J.; Matyjaszewski, K. *Macromolecules* **1998**, *31*, 8005.
- (38) Zhang, X.; Xia, J.; Matyjaszewski, K. *Macromolecules* **1998**, *31*, 5167.
- (39) Angot, S.; Murthy, K. S.; Taton, D.; Gnanou, Y. *Macromolecules* **1998**, *31*, 7218.
- (40) Ueda, J.; Kamigaito, M.; Sawamoto, M. *Macromolecules* **1998**, *31*, 6762.
- (41) Heise, A.; Nguyen, C.; Malek, R.; Hedrick, J. L.; Frank, C. W.; Miller, R. D. *Macromolecules* **2000**, *33*, 2346.
- (42) Matyjaszewski, K.; Miller, P. J.; Fossum, E.; Nakagawa, Y. *Appl. Organomet. Chem.* **1998**, *12*, 667.
- (43) Pyun, J.; Matyjaszewski, K. *Macromolecules* **2000**, *33*, 217.
- (44) Knischka, R.; Dietsche, F.; Hanselmann, R.; Frey, H.; Mülhaupt, R. *Langmuir* **1999**, *15*, 4751.
- (45) Lichtenhan, J. D.; Otonari, Y. A.; Carr, M. J. *Macromolecules* **1995**, *28*, 8435.
- (46) Omura, N.; Lubnin, A. V.; Kennedy, J. P. *ACS. Symp. Ser.* **1997**, *665*, 178.
- (47) Omura, N.; Kennedy, J. P. *Macromolecules* **1997**, *30*, 3204.
- (48) Majoros, I.; Marsalko, T. M.; Kennedy, J. P. *Polym. Bull.* **1997**, *38*, 15.
- (49) Hasegawa, I. *J. Sol-Gel Sci. Technol.* **1993**, *1*, 57.
- (50) Hasegawa, I.; Motojima, D. *J. Organomet. Chem.* **1992**, *441*, 373.
- (51) Ojima, I. In *The Chemistry of Organic Silicon Compounds*; Patai, S., Rappoport, Z., Eds.; Wiley: New York, 1989; p 1482.
- (52) Matyjaszewski, K.; Pintauer, T.; Gaynor, S. *Macromolecules* **2000**, *33*, 1476.

MA010814F